Search for nucleon-nucleon correlations in the proton spectral function of 208Pb

Bobeldijk, I; Blok, HP; van den Brink, HB; Dodge, GE; Hesselink, WHA; Jans, E; Kasdorp, WJ; Lapikas, L; van Leeuwe, JJ; Marchand, C

Published in:
Physics Letters B

DOI:
10.1016/0370-2693(95)00528-S

Publication date:
1995

ELSEVIER

22 June 1995

PHYSICS LETTERS B

Physics Letters B 353 (1995) 32–38

Search for nucleon-nucleon correlations in the proton spectral function of ^{208}Pb

I. Bobeldijk [a], H.P. Blok [b], H.B. van den Brink [b], G.E. Dodge [b], W.H.A. Hesselink [b], E. Jans [a], W-J. Kasdorp [a], L. Lapikás [a], J.J. van Leeuwe [a], C. Marchand [c], G. Onderwater [b], A. Pellegrino [b], M. van Sambeek [b], C.M. Spaltro [b], G. van der Steenhoven [a], J.J.M. Steijger [a], J.A. Templon [b], M.A. van Uden [a], R. de Vries [a], P.K.A. de Witt Huberts [a]

[a] *National Institute for Nuclear Physics and High-Energy Physics (NIKHEF, section K), P.O. Box 41882, 1009 DB Amsterdam, The Netherlands*

[b] *Department of Physics and Astronomy, Vrije Universiteit, De Boelelaan 1081, 1081 HV Amsterdam, The Netherlands*

[c] *Centre d'Etudes Nucléaires de Saclay, Departement d'Astrophysique, Physique des Particules, Physique Nucléaire et d'Instrumentation Associée/Service de Physique, F-91191 Gif-sur-Yvette, France*

Received 28 February 1995
Editor: J.P. Schiffer

Abstract

Cross sections for the reaction ^{208}Pb(e,e′p) have been measured with the continuous electron beam from the Amsterdam Pulse-Stretcher facility at NIKHEF-K. The spectral function has been extracted for protons with initial momenta of 300 to 500 MeV/c and binding energies up to 26 MeV. The data are compared to calculations with and without inclusion of nucleon-nucleon correlations. Mean-field predictions significantly underestimate the data and the discrepancy increases with binding energy. For transitions to the valence states the discrepancy is removed by introducing long-range correlations. Above the two-nucleon emission threshold long-range and short-range correlations reduce the discrepancy, but are insufficient to fully account for the measured strength.

Nucleon-nucleon (NN) correlations in atomic nuclei manifest themselves [1,2] in the spectral function at high nucleon momenta. To study NN-correlations in a heavy nucleus, the reaction ^{208}Pb(e,e′p) has been measured at initial proton momenta up to 500 MeV/c. For transitions corresponding to the removal of a proton from a valence orbital [3], the observed excess strength over the mean-field value appears to be mainly due to long-range correlations (LRC), whereas the calculated effect of short-range correlations (SRC) is considerably less. This is in agreement with the work of Müther and Dickhoff [4], who have demonstrated in their calculations of the ^{16}O spectral function, that SRC's hardly affect the valence transitions but grow in importance with increasing binding energy. A similar increase of high-momentum components with binding energy is observed in calculations of the spectral function of correlated nuclear matter [1,5]. In order to investigate the predicted binding-energy dependence of the high-momentum components of the spectral function we have measured the reaction ^{208}Pb(e,e′p) up to a proton binding energy of 26 MeV. The measurement was performed simultaneously with the one discussed in Ref. [3].

SSDI 0370-2693(95)00528-5

Since the experimental details of the present experiment have been presented in Ref. [3], only the most relevant features are repeated here. The experiment was carried out with the electron beam from the Amsterdam Pulse-Stretcher (AmPS) facility at NIKHEF-K [6]. The duty factor of the beam was about 50 %. The scattered electron and knocked-out proton were measured in coincidence by two magnetic spectrometers [7]. The central values of the experimentally probed missing momenta (p_m) (which in plane-wave impulse-approximation (PWIA) can be identified as the initial momenta of the ejected protons and for brevity are further referred to as momenta) are 145, 340, 400 and 495 MeV/c, where the acceptance covers a range of approximately 60 MeV/c. The data between 340 and 495 MeV/c were measured under kinematical conditions where the center of the acceptance corresponded to fixed values of the three-momentum transfer (q=221 MeV/c), energy transfer (ω=110 MeV) and proton kinetic energy ($T_{p'}$=100 MeV). The acceptance in excitation energy (E_x) of the residual nucleus was 18 MeV. A double-foil ^{208}Pb target with a total thickness of 87.4 ± 2.8 mg/cm^2 was used to double the luminosity and simultaneously maintain the E_x resolution at 180 keV. The total systematic uncertainty in the cross sections amounts to 6 %.

In Fig. 1 three spectra are displayed of the reduced cross section $\sigma_{\rm red}$ at mean momenta of 145, 340 and 495 MeV/c. The quantity $\sigma_{\rm red}$ is defined as the six-fold differential cross section divided by the off-shell electron-proton cross section σ_{ep}^{cc1} due to De Forest [8], and by the appropriate kinematical factor. Accidental coincidences have been subtracted in the spectra, the experimental phase space has been accounted for, and the spectra have been corrected for radiative processes [9]. It is evident from Fig. 1 that the relative importance of the continuum with respect to the valence transitions (E_x < 2.25 MeV) increases with increasing momentum.

Four experimental momentum distributions, $\rho(p_m, p')$, have been obtained by integrating $\sigma_{\rm red}$ over E_x in the ranges [−0.75,2.25], [2.25,7.25], [7.25,12.75] and [12.75,18.25] MeV. The boundary of 2.25 MeV represents the limit below which only discrete transitions to valence states in ^{207}Tl are observed, while the boundary of 7.25 MeV corresponds closely to the value of the two-nucleon emission thresholds (E_x^{pp}=7.37 MeV and E_x^{pn}=6.84 MeV). The third boundary of 12.75 MeV halves the remaining energy domain above E_x^{2N}. The momentum distributions (solid circles) in each range are displayed in Fig. 2 together with the data at low momentum obtained by Quint [10] (plus-marks).

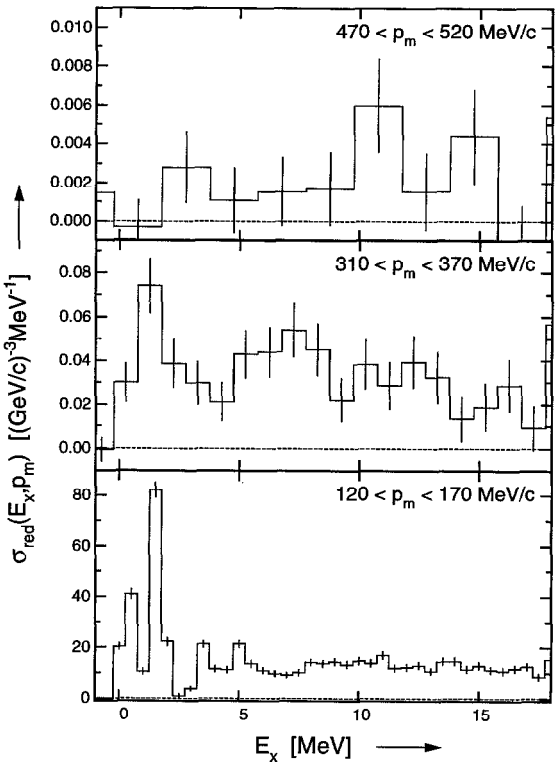

Fig. 1. Reduced cross section for the reaction ^{208}Pb(e,e'p) at average missing momenta of 145 MeV/c, 340 MeV/c and 495 MeV/c.

The data and the curves have been plotted as a function of the effective missing momentum $p_m^{\rm eff}$ [3,11] in order to account for the kinematical effect of Coulomb distortions on the momentum distributions. The solid curves in Fig. 2 represent a sum of mean-field momentum distributions obtained with distorted-wave impulse-approximation (CDWIA) calculations including Coulomb and proton distortions. The final-state interaction in these calculations is described with an optical model using the parameters from Ref. [12]. The employed bound-state wave functions are normalised mean-field wave functions generated in a Woods-Saxon potential. The root-mean square (RMS) radii of the valence orbitals ($3s_{\frac{1}{2}}$, $2d_{\frac{3}{2}}$,

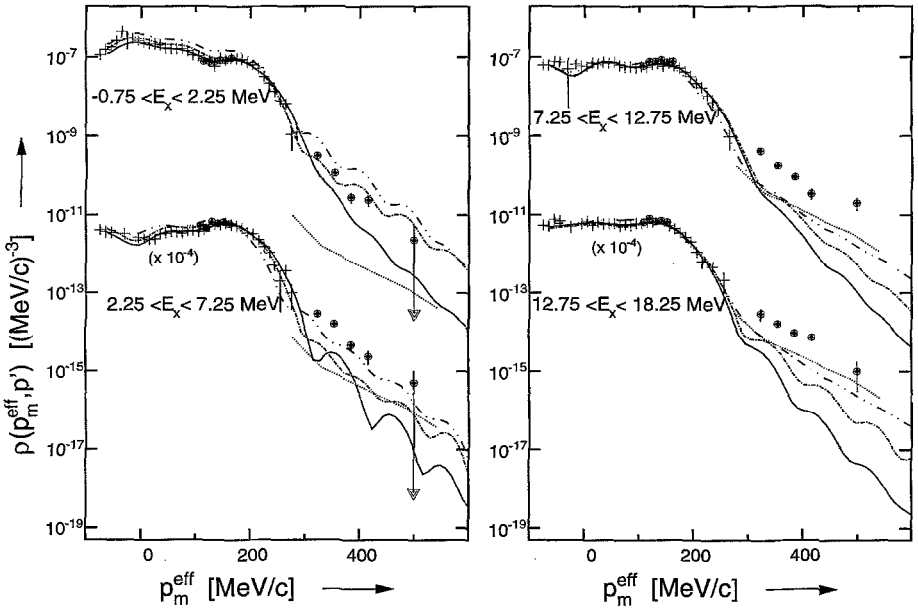

Fig. 2. Momentum distributions obtained from the reaction ^{208}Pb(e,e'p). The present data are represented by solid circles, while the plus-marks represent the data measured by Quint [10]. The solid curves represent CDWIA calculations employing mean-field wave functions. The dot-dashed curves are the result of CDWIA calculations including correlations as proposed by Mahaux and Sartor [13]. The dotted curves represent momentum-distributions extracted from the nuclear-matter spectral function of Ref. [5], modified for distortions (see text). The CDWIA calculations employing LDA wave functions [18] (see text) are represented by dash-doubledotted lines.

$1h_{\frac{11}{2}}$, $2d_{\frac{5}{2}}$ and $1g_{\frac{7}{2}}$) were obtained by fitting CDWIA curves to the data at low momentum (< 250 MeV/c) and low E_x (< 4 MeV) for each discrete transition. For the deeply bound orbitals that contribute in the present energy domain ($1g_{\frac{9}{2}}$, $2p_{\frac{1}{2}}$, $2p_{\frac{3}{2}}$, $1f_{\frac{5}{2}}$, $1f_{\frac{7}{2}}$ and $2s_{\frac{1}{2}}$), the RMS radius has been taken from Ref. [13]. For each E_x range the RMS radii were kept constant by adapting the radius parameter and the depth of the Woods-Saxon potential while reproducing the central binding energy of the interval.

As was also done in Ref. [3] the calculated CDWIA-cross sections are divided by the electron-proton cross section of McVoy-Van Hove σ_{ep}^{NR} [14] and by the appropriate kinematical factor to obtain momentum distributions. By using σ_{ep}^{NR} we compensate for the fact that the nucleon-current operator that is used in the CDWIA calculation is a non-relativistic expansion of the one that is used in σ_{ep}^{ccl}. The spectroscopic factor of each individual momentum distribution in the total summed momentum distribution is determined by fitting [9] the data obtained by Quint [10] up to a momentum of 250 MeV/c. In this procedure we neglected the difference between spin-orbit partners. The fit was performed separately for all four E_x ranges.

The mean-field calculations at high momentum are far below the data for all four E_x ranges. Moreover, the difference between the data and the mean-field calculations increases with increasing E_x. To investigate whether nucleon-nucleon correlations can explain this discrepancy, we also show in Fig. 2 the results of CDWIA calculations employing quasi-particle wave functions, as proposed by Mahaux and Sartor [13], with the same spectroscopic factors as in the mean-field case (dot-dashed curves). The quasi-particle wave functions have been obtained from the mean-field bound-state wave functions via multiplication by the energy-dependent modification function $G(r)$, and are renormalised afterwards [3]. The function $G(r)$ for the four E_x ranges is shown in Fig. 3. The curves clearly demonstrate the energy dependence of the quasi-particle effective mass, which is the square of $G(r)$. The quasi-particle effective mass is the product of the k-mass and the E-mass. The k-mass

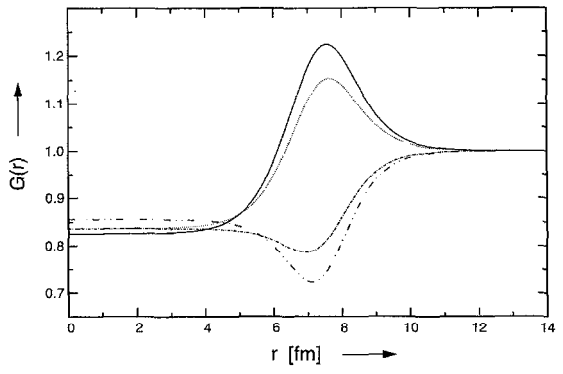

Fig. 3. The function $G(r)$, employed to convert mean-field wave functions in ^{208}Pb in the excitation energy ranges [−0.75,2.25] (solid), [2.25,7.25] (dotted), [7.25,12.75] (dot-dashed) and [12.75,18.25] MeV (dash-doubledotted) to quasi-particle wave functions, using the prescription of Mahaux and Sartor [13].

is determined by the momentum dependence of the self-energy. It is suppressed below unity at the nuclear interior, as is clearly visible in Fig. 3, by SRC effects arising from the NN-interaction and the exchange contribution to the mean-field potential. The E-mass is determined by the energy dependence of the self-energy and contains LRC-effects via the coupling of the hole state to low-lying excitations. Its effect at the nuclear surface changes from an enhancement at low energies to a quenching at larger energies.

The data for the valence transitions are well described by the calculations based on these quasi-particle wave functions, as was already observed in Ref. [3], where the conclusion was drawn that at low E_x the LRC contribution dominates over the SRC contribution. However, at $E_x > 2.25$ MeV the momentum distributions generated in this effective-mass approximation lie far below the data. Possibly, the contribution of SRC is insufficiently accounted for by employing this effective k-mass. Therefore we examined an infinite nuclear-matter spectral function [5] in which the high-momentum components are explicitly calculated on the basis of a realistic nucleon-nucleon interaction.

A comparison of the high-momentum components in nuclear matter with those of the finite nucleus ^{208}Pb is justified, since the transitions to the deeper-lying states in ^{207}Tl mainly probe the nuclear interior where the average nucleon density resembles that of nuclear matter. The momentum distributions are obtained from the nuclear-matter spectral function of Benhar et al. [5] by integration over the appropriate E_x bins. The spectral function is computed with correlated basis-function theory using the Urbana v_{14} NN-interaction [15] and a phenomenological three-nucleon force. Obviously, comparison of our data with the nuclear-matter momentum distribution is only meaningful above the Fermi momentum, since at low momentum the structure of the nuclear-matter spectral function cannot describe that of a finite system. In order to enable a comparison of the nuclear-matter results with the present ^{208}Pb data, we normalised the nuclear-matter spectral function to 82 protons. To account for final-state interaction and Coulomb distortions we have multiplied the resulting momentum distribution by a transparency factor of 0.21 and shifted it by 10.5 MeV/c towards smaller momenta. We have determined these values from a comparision of PWIA mean-field momentum distributions as a function of p_m with CDWIA calculations as a function of $p_m^{\rm eff}$, in the momentum range of 200 to 650 MeV/c. The dotted curves in Fig. 2 represent the nuclear-matter momentum distributions.

The calculated short-range correlations clearly gain in importance with energy as is already seen in the left panel of Fig. 2. This trend continues with increasing E_x as demonstrated in the right panel of Fig. 2, where the nuclear-matter momentum distributions move towards the data. In order to further investigate the importance of SRC-effects, these need to be included in a calculation for finite systems containing also LRC-effects.

Van Neck et al. [18] have performed such a calculation by evaluating the spectral function for ^{208}Pb within the framework of the local-density approximation (LDA), starting from the nuclear-matter spectral function at various densities [16,17]. The computed spectral function is decomposed into a single-particle part and a "correlated" part. The former part describes the broadening and depletion of the quasi-hole states. It is provided in the form of wave functions and spectroscopic factors for all sixteen hole states. The wave functions were constructed by a Hartree-Fock calculation with the Skyrme-3 force and modulated with a nuclear-radius dependent factor to account for SRC-effects. Moreover, surface vibrations, i.e. LRC-effects, are included in the wave functions via the prescription of Mahaux and Sartor [13] for the E-mass. The energy

distribution of the spectroscopic factors of each hole-state was calculated in LDA. It peaks at the Hartree-Fock single-particle energy and has a broadening determined by the nuclear-matter spectral functions. We employed these single-particle wave functions to calculate CDWIA momentum distributions, which are then multiplied by the corresponding spectroscopic factors.

The "correlated part" of the spectral function is calculated in LDA from the same nuclear-matter spectral function [5] that is used before. It is supplied as a momentum distribution and a spectroscopic factor for the E_x bins [7.25,12.75] and [12.75,18.25] MeV. At lower energy this part of the spectral function does not contribute. The correlated momentum distributions are multiplied by the given spectroscopic factors. Distortions were treated in the same way as above for the nuclear-matter momentum distribution by applying the transparency factor and the momentum shift. The dash-doubledotted curves in Fig. 2 represent the sum of the single-particle and correlated momentum distribution.

Although the LDA-CDWIA calculations include LRC-effects as prescribed by Mahaux and Sartor, they lie above the data in the first E_x bin over the whole momentum range. This is partly due to the size of the Hartree-Fock spectroscopic factors, which results in an overestimate of the data at low momentum (< 250 MeV/c) and low E_x (< 2.25 MeV). In the second E_x bin the calculations in LDA are close to the data. This is not true any longer for the data above E_x^{2N}, where the LDA-momentum distributions are far below the data.

In order to quantify the increase with energy of the measured high-momentum components, with respect to the various described calculations, we calculated the function $R(E_x)$. It is defined as the ratio of the measured or calculated spectral function integrated over the momentum range [300,500] MeV/c relative to the corresponding mean-field value. The ratio $R(E_x)$ has been plotted in Fig. 4. The measured increase of high-momentum strength with energy relative to the mean-field predictions is clearly demonstrated. The SRC-effects are rapidly gaining in importance with E_x as shown in Fig. 4 where the calculated strength based on the nuclear matter and the LDA momentum distributions is closer to the data than the other calculations. However, a substantial discrepancy remains

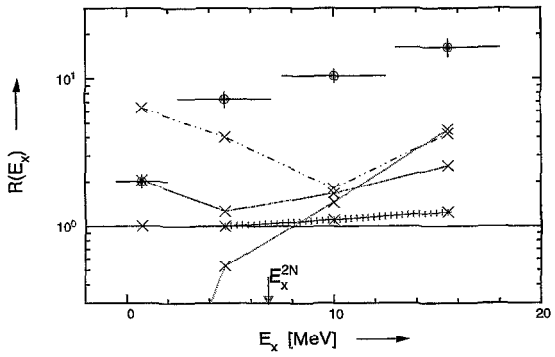

Fig. 4. The ratio $R(E_x)$ (see text) for four different energy ranges indicated by the horizontal error bars. The solid circles represent the present data. The solid curve is the mean-field ratio. The theoretical values for the $R(E_x)$ with quasi-particle, nuclear matter and LDA-momentum distributions are represented by the dot-dashed, dotted and dash-doubledotted curves, respectively. The dashed curve shows the effect of an enhanced ratio of transverse/longitudinal structure functions above E_x^{2N}.

between the data and all described calculations at high momenta and above E_x^{2N}.

We have considered rescattering processes as a possible cause for the large strength observed above E_x^{2N}. In Ref. [24] a method is described to evaluate the probability for those events of the type (e,e'p')(p',p) that fall within the acceptance of the spectrometer. Based on this method we have calculated the contribution of these processes to the presently measured cross sections above E_x^{2N} to be less than 2%. The smallness of the contribution is due to the limited kinematical acceptance of the spectrometers and Pauli-blocking effects for the other nucleons involved. Even if the Pauli-blocking restriction is omitted the rescattering contribution stays below 5%. Clearly rescattering is excluded as a cause for the observed strength of the high-momentum components in the present energy domain.

Thusfar, the treatment of the reaction mechanism was restricted to the coupling of a virtual photon to one proton. Going beyond this framework of a one-body current operator we have investigated whether two-body currents could contribute significantly in this energy domain. As no exact calculations are available, we performed CDWIA calculations including a phenomenological estimate of two-body currents effects derived from recent (e,e'p) experiments [19] on ^{6}Li [20], ^{10}B [21], ^{12}C [22] and ^{40}Ca [23]. In

these experiments an enhancement of the ratio (η) of Transverse (W_T) and Longitudinal (W_L) structure functions (normalised by their impulse approximation values) was observed above E_x^{2N}. The effect was attributed to the onset of two-nucleon emission [19], which is a dominantly transverse process.

As the experimentally determined value of η has the same behaviour as a function of energy with respect to E_x^{2N} for all nuclei investigated [19], we used these same values of η (1.17 and 1.36) in our CDWIA calculations for ^{208}Pb in the E_x ranges [7.25,12.75] and [12.75,18.25] MeV, respectively. In the absence of theoretical estimates and experimental data for the momentum dependence of the quantity η we had to assume that the value of η obtained in parallel-kinematics at low momenta (< 250 MeV/c) can be applied in the present non-parallel kinematics at high momenta (< 500 MeV/c). In the latter kinematics the transverse current component also enters via the longitudinal-transverse interference structure function (W_{LT}).

The inclusion of η results in a minor increase in comparison to the mean-field calculations, as shown by the curve composed of plus-marks in Fig. 4. Although this indicates that the effect of two-body currents is insufficient to explain the data, we note that a more definite conclusion on the role of two-body currents requires explicit calculations. Experimentally the role of two-body currents has been investigated with the complementary reaction ^{208}Pb(γ,p), the results of which will be reported in a forthcoming paper [25]. Whereas the reaction ^{208}Pb(e,e'p) is dominantly longitudinal (the virtual-photon polarization is 0.88), the reaction (γ,p) is of purely transverse nature and thus expected to be more sensitive to two-body currents.

In summary, an electron-induced proton knock-out experiment on ^{208}Pb has been carried out that probes initial proton momenta from 300 to 500 MeV/c and binding energies up to 26 MeV. The data have been compared to CDWIA calculations employing mean-field wave functions, quasi-particle wave functions generated in an effective-mass approximation, and wave functions that are computed in the local-density approximation starting from a nuclear-matter spectral function. A significant discrepancy between the data and the mean-field prediction is observed, which increases with energy. For the valence transitions ($E_x < 2.25$ MeV) long-range correlations can explain the discrepancy, but at larger excitation energies their influence decreases. The calculated contribution of short-range correlations grows rapidly with E_x, although at $E_x > E_x^{2N}$ their inclusion is insufficient to properly describe the measured high-momentum components. The remaining discrepancy might be due to the effects of two-body currents as the cross sections at high momenta receive significant transverse contributions through the longitudinal-transverse interference structure function (W_{LT}). Although an initial estimate indicates that the effects of two-body currents are small, more explicit calculations are called for in order to achieve a proper understanding of the ^{208}Pb(e,e'p) data at high momenta and large binding energies.

We would like to thank Dr. O. Benhar for providing the nuclear-matter spectral function and Dr. D. van Neck for supplying wave functions and spectroscopic factors in the local-density approximation. The work described in this paper is part of the research programme of the "Stichting voor Fundamenteel Onderzoek der Materie (FOM)", which is financially supported by the "Nederlandse Organisatie voor Wetenschappelijk Onderzoek (NWO)".

References

[1] W.H. Dickhoff, Phys. Reports 242 (1994) 119.
[2] C. Mahaux and R. Sartor, Nucl. Phys. A 546 (1992) 65c.
[3] I. Bobeldijk et al., Phys. Rev. Lett. 73 (1994) 2684.
[4] H. Müther and W.H. Dickhoff, Phys. Rev. C 49 (1994) R17.
[5] O. Benhar, A. Fabrocini and S. Fantoni, Nucl. Phys. A 505 (1989) 267.
[6] P.K.A. de Witt Huberts, Nucl. Phys. A 553 (1993) 845c.
[7] C. de Vries et al., Nucl. Instrum. Methods 223 (1984) 1.
[8] T. de Forest Jr., Nucl. Phys. A 392 (1983) 232.
[9] J.W.A. den Herder et al., Nucl. Phys. A 490 (1988) 507.
[10] E.N.M. Quint, Ph.D. thesis, University of Amsterdam (1988).
[11] Y. Jin, H.P. Blok and L. Lapikás, Phys. Rev. C 48 (1993) R964.
[12] H.P. Blok, L.R. Kouw, J.W.A. den Herder, L. Lapikás and P.K.A. de Witt Huberts, Phys. Lett. B 198 (1987) 4.
[13] C. Mahaux and R. Sartor, Adv. Nucl. Phys. 20 (1991) 1.
[14] H.P. Blok, Proc. Int. Conf., Trieste, 1993.
[15] I.E. Lagaris and V.R. Pandharipande, Nucl. Phys. A 359 (1981) 331.
[16] I. Sick, S. Fantoni, A. Fabrocini and O. Benhar, Phys. Lett. B 323 (1994) 267.

[17] O. Benhar, A. Fabrocini, S. Fantoni and I. Sick, Nucl. Phys. A 579 (1994) 493.
[18] D. van Neck, A.E.L. Dieperink and E. Moya de Guerra, submitted to Phys. Rev. C (1995).
[19] G. van der Steenhoven, Nucl. Phys. A 527 (1991) 17c.
[20] J.B.J.M. Lanen et al., Phys. Rev. Lett. 64 (1990) 2250.
[21] L.J. de Bever, Ph.D. thesis, University of Utrecht (1993).
[22] G. van der Steenhoven et al., Nucl. Phys. A 484 (1988) 445.
[23] H.J. Bulten, Ph.D. thesis, University of Utrecht (1992).
[24] G.P. Capitani et al., Il Nuovo Cimento A 85 (1985) 37.
[25] I. Bobeldijk et al., to be submitted to Phys. Lett. B (1995).